BIOCHEMISTRY
including biophysical chemistry & molecular biology
Article

Biochemistry **2009,** *48,* 9437–9447 9437
DOI: 10.1021/bi900909g

Conserved Polar Residues Stabilize Transmembrane Domains and Promote Oligomerization in Human Nucleoside Triphosphate Diphosphohydrolase 3†

Keith J. Gaddie and Terence L. Kirley*

Department of Pharmacology and Cell Biophysics, College of Medicine, University of Cincinnati, P.O. Box 670575, Cincinnati, Ohio 45267-0575

Received May 29, 2009; Revised Manuscript Received September 9, 2009

ABSTRACT: Polar residues play essential roles in the functions of transmembrane helices by mediating and stabilizing their helical interactions. To investigate the structural and functional roles of the conserved polar residues in the N- and C-terminal transmembrane helices of human nucleoside triphosphate diphosphohydrolase 3 (NTPDase3) (N-terminus, S33, S39, T41, and Q44; C-terminus, T490, T495, and C501), each was singly mutated to alanine. The mutant proteins were analyzed for enzymatic activities, glycosylation status, expression level, and Triton X-100 detergent sensitivity. The Q44A mutation decreased Mg-ATPase activity by approximately 70% and abolished Triton X-100 detergent inhibition of Ca-dependent nucleotidase activities while greatly attenuating Triton X-100 inhibition of Mg-dependent nucleotidase activities. The polar residues were also mutated to cysteine, singly and in pairs, to allow a disulfide cross-linking strategy to map potential inter- and intramolecular hydrogen bond interactions. The results support the centrality of Q44 for the strong intermolecular interactions driving the association of the N-terminal helices of two NTPDase3 monomers in a dimer, and the possibility that T41 may play a role in the specificity of this interaction. In addition, S33 and C501 form an intramolecular association, while S39 and T495 may contribute to helical interactions involved in forming higher-order oligomers. Lastly, Tween 20 substantially and selectively increases NTPDase3 activity, mediated by the transmembrane helices containing the conserved polar residues. Taken together, the data suggest a model for putative hydrogen bond interactions of the conserved polar residues in the transmembrane domain of native, oligomeric NTPDase3. These interactions are important for proper protein expression, full enzymatic activity, and susceptibility to membrane perturbations.

Human nucleoside triphosphate diphosphohydrolase 3 (human NTPDase3)[1] is a member of a family of ecto-enzymes that are characterized by their ability to hydrolyze extracellular and intraluminal nucleoside di- and triphosphates in the presence of divalent cations (*1*). There are eight members in the human family of NTPDases. NTPDase1−3 and -8 are expressed on the cell surface and hydrolyze extracellular nucleotides, while NTPDase4−7 hydrolyze intraluminal nucleotides (*2*, *3*). NTPDase1−4, -7, and -8 are membrane-bound glycoproteins with a transmembrane (TM) helix near both their N- and C-termini, and a large extracellular domain containing five conserved disulfide bonds and the enzyme active site (*4*). NTPDase5 and -6 are found in intracellular membrane organelles but can also be secreted as soluble enzymes upon cleavage of their respective N-terminal signal sequences (*5*, *6*). The NTPDases are also distinguished from one another by their nucleotide substrate specificities and catalytic properties (*7*), with those enzymes targeted to intracellular organelles being inefficient nucleoside triphosphatases (poor hydrolysis of ATP). Although the functions of the NTPDases are still under investigation, it is known that the cell surface members of this enzyme family hydrolyze extracellular nucleotides acting as agonists at purinergic receptors to modulate many physiological processes, including blood clotting, pain perception, and smooth muscle contraction (*8*).

Many site-directed mutagenesis experiments (mostly performed on NTPDase3) have demonstrated the importance of conserved residues in the extracellular domain of the NTPDases (*9*), and a recently published crystal structure of the extracellular portion of rat NTPDase2 has confirmed and extended those site-directed mutagenesis results (*10*). In addition, previous studies from the same laboratory that determined the crystal structure of the extracellular portion of rat NTPDase2 demonstrated that the extracellular portions of rat NTPDase1−3 could be refolded from bacterial inclusion bodies to soluble, highly active nucleotidases (*11*). However, consistent with studies involving expression of the soluble, extracellular portion of CD39/NTPDase1 (*12*), the specific activity of the bacterially expressed and refolded NTPDases [approximately 200 μmol mg^{-1} min^{-1} = 12000 μmol mg^{-1} h^{-1} (*11*)] was substantially lower than what was reported for a purified, full-length NTPDase (rabbit NTPDase2) (*13*), which has a specific activity of approximately 400000 μmol mg^{-1} h^{-1}.

[†] This work was supported by National Institutes of Health R01 Grant HL72382/HL72382-S1 to T.L.K.

*To whom correspondence should be addressed: Department of Pharmacology and Cell Biophysics, College of Medicine, University of Cincinnati, P.O. Box 670575, Cincinnati, OH 45267-0575. Phone: (513) 558-2353. Fax: (513) 558-9969. E-mail: terry.kirley@uc.edu.

[1] Abbreviations: NTPDase3, nucleoside triphosphate diphosphohydrolase 3; TM, transmembrane; TMD, transmembrane domain; BME, β-mercaptoethanol; DTT, dithiothreitol; CuPhen, copper phenanthroline; MalPEG, maleimide polyethylene glycol 5000; MOPS, 3-(*N*-morpholino)propanesulfonic acid; HEPES, *N*-(cyclohexyl)-2-aminoethanesulfonic acid; SDS−PAGE, sodium dodecyl sulfate−polyacrylamide gel electrophoresis.

Most studies regarding the role of the transmembrane domain (TMD) of the membrane-bound, cell-surface NTPDases have focused on oligomerization. The predominant, active form of these enzymes appears to be a dimer, although higher-order oligomers are also observed, and the soluble NTPDases (which lack TMDs) are monomeric (*14*−*16*). However, no structural data exist, and no site-directed mutagenesis studies have been performed to perturb and analyze helix interactions in the TMD of NTPDase3. These interactions are likely different from those of the other membrane-bound NTPDases, since other NTPDases do not have the conserved polar residues found in NTPDase3 and mutated in this study.

Generally, TM α-helices consist of 20−30 hydrophobic amino acids that have a central region rich in aliphatic residues and phenylalanines, and short border regions enriched with tryptophan and tyrosine (*17*). Strongly polar residues such as arginine, asparagine, aspartic acid, glutamic acid, glutamine, histidine, and lysine are under-represented in TM helices (*18*, *19*), and mutations of these residues often cause adverse effects on enzyme function, suggesting conserved structural and functional roles (*20*−*22*). The most direct method for determining the hydrogen bonding pattern of the conserved polar residues in the TMD of NTPDase3 is crystallization of the full-length enzyme. Several membrane-bound enzymes have been crystallized (*23*), revealing the hydrogen bonding pattern of the polar residues in the TM helices (*24*). However, very few crystal structures of membrane proteins exist, and no crystal structure has been determined for any full-length NTPDase. Therefore, alternative approaches from which the three-dimensional organization of the TM helices may be inferred must be applied.

The introduction of cysteine residues at specific locations in the TM helices by site-directed mutagenesis and subsequent oxidative cross-linking has proven to be a useful method for determining spatial proximity, orientation, and flexibility of TM helices (*25*−*33*). A better understanding of the organization of the TMD of the NTPDases, specifically how the N- and C-terminal TM helices interact within and/or between monomers, is essential for a better understanding of enzyme function and its modulation by oligomerization and membrane perturbation. In this study, we demonstrate the importance of the conserved TM polar residues for optimal protein expression and enzymatic activity of NTPDase3, presumably mediated by polar amino acid hydrogen bond TM helix interactions necessary for proper protein processing and folding. Furthermore, we developed a model of putative helical hydrogen bond interactions based on cysteine substitution pairs and oxidative cross-linking of these residues in the NTPDase3 TM helices. The Q44 residue, which is conserved in all NTPDase3 sequences, is located at the interface of the N-terminal TM helix and the extracellular portion of NTPDase3 and appears to be the "linchpin" of the intermolecular TM interactions, driving association of the N-terminal TM helices of two monomers to form the native, dimeric NTPDase3. We also discovered that the detergent, Tween 20, unlike most other detergents that perturb the membrane and decrease NTPDase3 activity, increases NTPDase3 activity. This effect is not seen in the closely related human NTPDase1 and NTPDase2 enzymes and appears to be mediated by favorable effects of the detergent on oligomerization of NTPDase3 mediated by the TM helices containing the conserved polar residues unique to NTPDase3.

MATERIALS AND METHODS

Site-Directed Mutagenesis of NTPDase3. The QuikChange site-directed mutagenesis kit (Stratagene) was used to mutate NTPDase3 in the pcDNA3 expression vector as previously described (*34*). Fisher Oligo produced the synthetic oligonucleotide primers needed to engineer each mutant. The sense primers used for the mutagenesis are as follows: S33A, 5′-GGTGG TCTTG CTTGTGGCTATTGT GGTAC TTGTG-3′; S39A, 5′-GAGTAT TGTGGTAC TTGTGGCTATCACT GTCAT CCAG ATCC-3′; T41A, 5′-CTTGT GAGTATCGCTGTCAT CCAGA TCCA CAAGC-3′; Q44A, 5′-GTGA GTATC ACTGT CATCGCGATCCA CAAGC AAGAGG-3′; T490A, 5′-CCTG TCTTT GTGGGCGCCCTCG CTTT CTTC-3′; T495A, 5′-CCTCG CTTT CTTCACAGCAGCGG CAGC CTTG-3′; C501A, 5′-CACA GCGG CAGC CTTGCTGCTCTGGCATTT CTTGC ATAC-3′; S33C, 5′-CTTGG TGGTCT TGCTT GTGTGTATTGTG GTACT TGTGAG-3′; S39C, 5′-GTGAGTATTGTGGTACTTGTGTGTATCACTGTCATCCAGATC-3′; T41C, 5′-GTGGT ACTTGT GAGTATCTGTGTCATCC AGATCC ACAAG-3′; Q44C, 5′-CTTGTG AGTATC ACTGT CATCTGTATCCACAAGCAAGAGGTCCTC-3′; T490C, 5′-CACCT GTCTTT GTGGGCTGCCTCGCTT TCTTCA CAGC-3′; T495C, 5′-CACCC TCGCTT TCTTCTGCGCGGCA GCCTTG CTGTC-3′; Q44C/S39C, 5′-GTGA GTATTGT GGTACTT GTGTGTATCACT GTCATCTGTATC-3′; Q44C/T41C, 5′-GTGGTA CTTGTG AGTATCTGTGTCATCTGTATCCACAAG-3′.

The altered codons are underlined, and the complementary antisense oligonucleotides also required for mutagenesis are not shown. The polar residue to alanine substitution mutants were made in the "wild-type like" C10S NTPDase3 background, and the single- and double-cysteine mutants were made in the "free sulfhydryl-less" C10S/C501S/C509S NTPDase3 background [which has enzymatic properties similar to those of WT C10S (*35*)], except for the S33C/C501 mutant which was made in the C10S/C509S NTPDase3 background [also having enzymatic properties similar to those of WT C10S (*35*)]. DNA Analysis, LLC, sequenced the resulting cDNA constructs to verify the presence of the desired mutation and the absence of any unwanted changes.

Transient Transfection and Preparation of COS-1 Cell Membranes. COS-1 cells were grown in Dulbecco's modified Eagle's medium (DMEM) with 10% bovine serum and a 2% mixture of antibiotics and antimycotics (Invitrogen). The cells were transfected with 4 μg of plasmid DNA (or empty pcDNA3 vector as a control) per 100 mm cell culture plate using Lipofectamine and PLUS reagents (Invitrogen) as previously described (*36*). The COS-1 cells were harvested approximately 48 h post-transfection. The crude cell membrane preparations were obtained as previously described (*36*).

Protein Assay. Protein concentrations were determined using the Bio-Rad protein assay reagent with the modifications of Stoscheck (*37*). Bovine serum albumin was used as a standard.

Nucleotidase Assay of Transfected COS-1 Cells Expressing NTPDase3. Nucleotidase activities were determined by measuring the amount of inorganic phosphate (P_i) released from nucleotide substrates (Sigma) at 37 °C using modifications of the technique of Fiske and Subbarow (*38*), as previously described (*34*). Either 5 mM $MgCl_2$ or 5 mM $CaCl_2$ (each in 20 mM MOPS 7.1 buffer) was used for cation-dependent nucleotidase activities. The reactions were initiated by the addition of nucleotide to a final concentration of 2.5 mM in the 0.3 mL assay solutions. Hydrolysis was allowed to proceed for 30 min or 1 h, depending on the substrate used. The activities were corrected for pcDNA3/COS-1 cell background (membranes from COS-1 cells transfected with an empty vector), as well as differences in expression levels as determined by quantitative Western blotting of each sample.

Triton X-100 Nucleotidase Assays. In some experiments, COS-1 cell crude membrane protein (0.05 mg/mL) was solubilized in 1% Triton X-100 and 25 mM MOPS buffer (pH 7.1) at 22 °C for 10 min with occasional vortexing. In most experiments, nucleotidase activities were measured by dilution of COS membranes into assay solutions containing 0.1% Triton X-100, using either 5 mM $CaCl_2$ or 5 mM $MgCl_2$ (each in 20 mM MOPS 7.1 buffer) and nucleotide at a final concentration of 0.25 mM, using a malachite green phosphate assay (*39*), due to the interference of Triton X-100 with the modified Fiske and Subbarow assay described above. After addition of nucleotide to start the reaction, hydrolysis was allowed to proceed for 8 min (Ca-ATPase), 16 min (Ca-ADPase), 16 min (Mg-ATPase), or 32 min (Mg-ADPase) at 37 °C. The absorbance at 630 nm was measured to determine the amount of inorganic phosphate (P_i) released.

SDS−PAGE and Western Blotting. Precast 10-well or 15-well 4 to 15% gradient mini-gels (Bio-Rad) were used to resolve aliquots of crude membrane proteins (0.5−2 μg, depending on the sample and the experimental purpose), usually after boiling for 5 min in SDS sample buffer containing 30 mM dithiothreitol (DTT). Following SDS−PAGE, the proteins were electro-transferred to Immun-Blot PVDF membrane (Bio-Rad) for 3 h at 33 V in cold 10 mM CAPS-NaOH (pH 11). After transfer, the PVDF membrane was incubated for 1 h in blocking solution [5% nonfat dry milk in Tris-buffered saline (TBS)] at room temperature (22 °C) and then incubated overnight at room temperature in blocking solution containing 0.02% sodium azide and a 1:5000 dilution of rabbit polyclonal primary antisera of KLH1, generated against the cytoplasmic C-terminal peptide (amino acid residues 515−529) of human NTPDase3 (*15*). After the blot was washed in a TBS/0.05% Tween 20 solution, a goat anti-rabbit HRP-conjugated secondary antibody (Pierce) was applied at a 1:4000 dilution for 1 h at room temperature followed by washing and application of the Pierce SuperSignal West Dura Extended Duration Substrate to the PVDF membrane for 5 min to detect immunoreactivity by chemiluminescence. Chemiluminescence was recorded and quantified using a FluorChem IS-8800 system (Alpha Innotech).

Oxidative Cross-Linking and Alkylation of Cysteine. Copper phenanthroline (CuPhen) was used as the oxidative cross-linker to form disulfides from pairs of free cysteine sulfhydryls. We prepared the reagent just before use by combining cupric sulfate and 1,10-phenanthroline (Sigma) at a 1:3 ratio in 20% ethanol as described previously (*40*). Cysteine-substituted COS-1 cell crude membrane protein (0.1 mg/mL) was cross-linked with a final concentration of 0.5 mM CuPhen in 50 mM HEPES (pH 7.5) at 37 °C for 20 min. For samples directly analyzed by SDS−PAGE, the reactions were stopped via addition of an equal volume of nonreducing SDS loading buffer containing 20 mM EDTA. For samples alkylated with maleimide polyethylene glycol 5000 (MalPEG), the cross-linking reaction was stopped with 0.5 volume of a solution to yield final concentrations of 20 mM EDTA and 1% SDS in 20 mM HEPES (pH 7.5). The samples were incubated at room temperature (22 °C) for 10 min with occasional vortexing, followed by the addition of MalPEG to a final concentration of 5 mM. The samples were alkylated at room temperature for 20 min with occasional vortexing, and the reaction was stopped via addition of an equal volume of nonreducing SDS−PAGE loading buffer. The samples were then heated at 60 °C for 10 min and loaded onto a gel for SDS−PAGE followed by Western blot analysis as described above.

Deglycosylation. Deglycosylation was performed using Endo H (New England Biolabs) according to the manufacturer's instructions, as previously described (*4*). Briefly, COS-1 cell crude membrane protein was solubilized with 0.2% Triton X-100 containing 1 mM EDTA for 30 min at 22 °C. The solubilized samples were then centrifuged in a Beckman air-driven centrifuge for 20 min at 100000*g*. The supernatant was combined with 10× glycoprotein denaturing buffer (to yield final concentrations of 0.5% SDS and 1% β-mercaptoethanol) and boiled for 10 min. After cooling to room temperature (22 °C), each sample was combined with the appropriate reaction buffer (NEBuffer G5), aliquoted, and incubated with or without (controls) Endo H at 37 °C for 1 or 3 h. After incubation, the samples were combined with SDS sample buffer containing 100 mM DTT, run on an SDS−PAGE gel, and subjected to Western blot analysis as described above.

NTPDase3 Nucleotidase Assays in the Presence of Tween 20. COS-1 cell crude membrane protein (0.25 μg/mL) was preincubated for 5 min at 37 °C in 0.1% Tween 20 and 5 mM $MgCl_2$ or 5 mM $CaCl_2$ (each in 20 mM MOPS 7.1 buffer). After addition of nucleotide at a final concentration of 0.25 mM to start the reaction, hydrolysis was allowed to proceed for 5 min (Ca-ATPase), 10 min (Ca-ADPase), 10 min (Mg-ATPase), or 20 min (Mg-ADPase) at 37 °C. Nucleotidase activities were measured using a malachite green phosphate assay (*39*). The absorbance at 630 nm was measured to determine the amount of inorganic phosphate (P_i) released.

RESULTS

Rationale for Selection and Analysis of TM Polar Residue Mutants. Multiple sequence alignments of the N- and C-terminal TM helices of all known NTPDase3 sequences to date revealed complete conservation of polar residues Ser33 and Gln44, strong conservation of Thr41 and Cys501, and a much more limited degree of conservation for Ser39, Thr490, and Thr495 (Figure 1A). Helical wheel predictions of the TM helices revealed that three pairs of polar residues, namely, Q44 and T490, S39 and T495, and S33 and C501, are at approximately the same depth in the membrane and located on the same face of the α-helices (Figure 1B). This suggests that each pair has the potential for inter- or intramolecular hydrogen bonding (Figure 1C).

Characterization of the NTPDase3 Polar Residue to Alanine Mutants. To explore the structural and/or functional significance of the conserved polar residues in the N-terminal (S33, S39, T41, and Q44) and C-terminal (T490, T495, and C501) TM helices of NTPDase3, we utilized site-directed mutagenesis to singly substitute an alanine residue (a nonpolar amino acid) for each of the polar residues and expressed the mutants in COS-1 cells. The "wild-type-like" C10S NTPDase3, denoted as WT (C10S) throughout this paper, was used as the background for these mutations to eliminate the artificial dimerization via oxidation of Cys10 which is observed when homogenizing COS membranes expressing WT human NTPDase3 (*35*). The mutants were characterized for proper glycosylation and delivery to the cell surface in their native oligomeric state, as well as enzymatic activities, expression level, and sensitivity to Triton X-100 inhibition (see Table 1). As shown in Table 1, alanine substitution caused a significant and substantial decrease in the expression

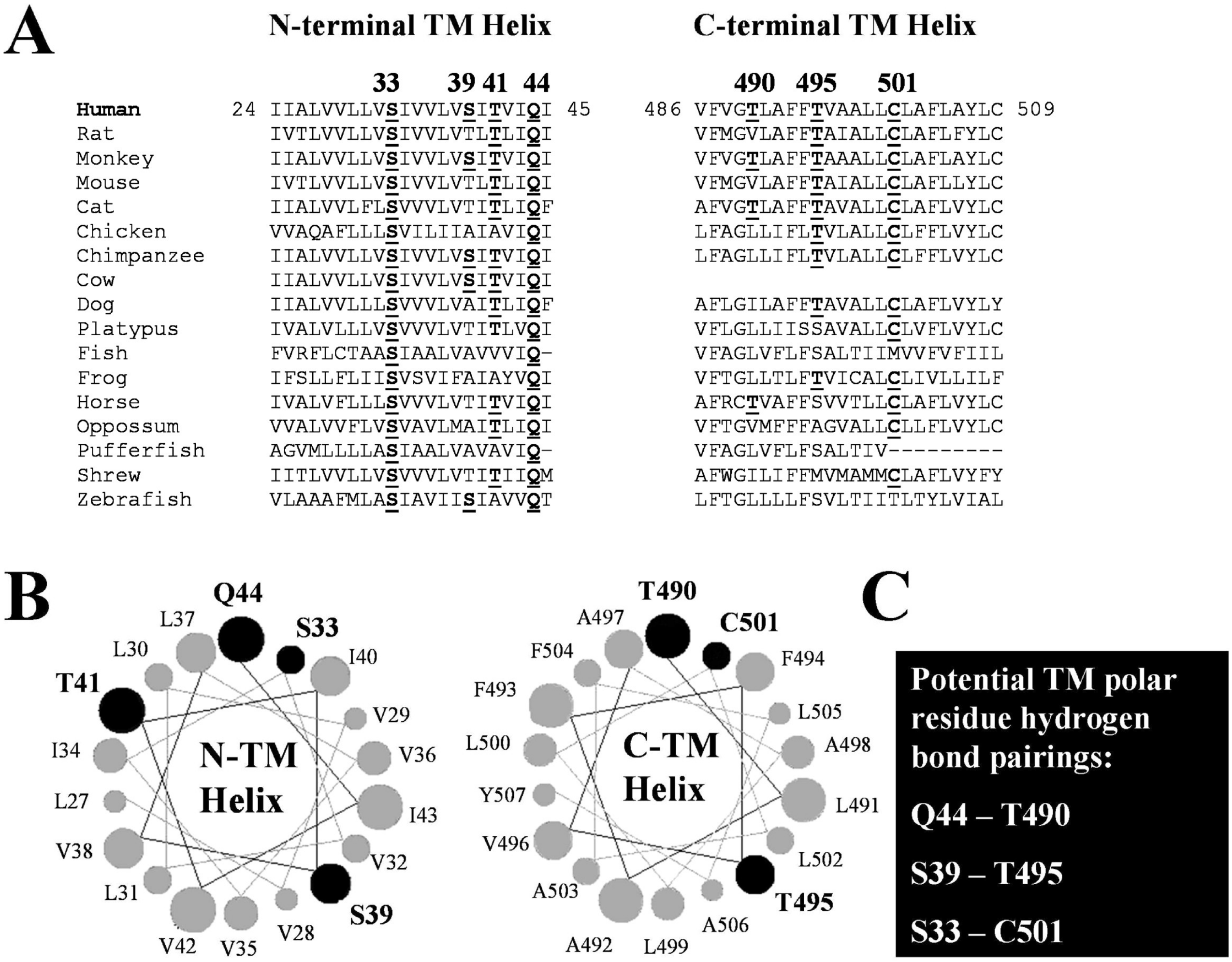

FIGURE 1: Rationale for NTPDase3 mutations generated and analyzed in this study. (A) Multiple sequence alignment of the N- and C-terminal TM helices in NTPDase3. The polar residues present in human NTPDase3 which were mutated are shown in bold and underlined. The sequence in GenBank for the cow NTPDase3 terminates prior to the C-terminal TM helix and is therefore not known and not shown in the figure. (B) Helical wheel analysis of human NTPDase3 TM helices. The polar TM amino acids are represented by filled black circles. The helices are depicted as viewed from the extracellular side of the cell membrane, with the size of the circles (representing the amino acids) decreasing with an increase in the distance from the cell surface. (C) Potential TM polar residue hydrogen bond pairings. On the basis of the positions on the helical wheel diagram, Q44, S39, and S33 on the N-terminal TM helix are predicted to be on the same face and at the same depth as T490, T495, and C501 on the C-terminal TM helix (B), respectively. Note that intramolecular or intermolecular bonds (or both, in the case of Q44 which can form two hydrogen bonds) are possible for these polar residues present in the NTPDase3 dimer, which includes two N-terminal and two C-terminal TM helices.

level of S33, S39, Q44, T495, and C501 mutants as compared to WT (C10S) NTPDase3. After correction for expression level, many of the mutants had specific enzymatic activities similar to that of the WT (C10S) enzyme (see Table 1). However, T490A and T495A had reduced activity (~70% of the Mg-ATPase activity), and the activity of the Q44A mutant was reduced to ~30% of the Mg-ATPase activity of the WT (C10S) NTPDase3 (Table 1).

Because of the significant decrease in expression level and changes in nucleotide hydrolysis as compared to WT (C10S), possible changes in processing and trafficking of the mutants to the cell surface were examined. During studies that established the location of five extracellular disulfide bonds in human NTPDase3, Endo H deglycosylation analysis was shown to be a simple and reliable assay for proper protein processing and delivery to the cell surface (*4*). WT (C10S) and mutant enzymes all migrate at approximately 80 kDa, and like WT (C10S), all exhibit only a small shift in the electrophoretic mobility upon treatment with Endo H, with little to no protein completely deglycosylated by Endo H to migrate at the core protein size of 59 kDa (data not shown). This indicates that the mutant proteins were properly glycosylated and suggests they were normally trafficked to the cell surface.

To monitor the effects of alanine substitution on monomeric NTPDase3, the mutant proteins were treated with Triton X-100, a detergent known to cause dissociation of NTPDase3 oligomers into monomers. The Triton X-100-induced inhibition of WT (C10S) and most mutants is obvious, especially for the Mg-dependent activities, which are more sensitive to detergent inhibition than the Ca-dependent activities (Figure 2A), consistent with previous results (*35*). As seen in Figure 2A, Q44A, unlike the WT (C10S) and other polar residue mutants, is relatively insensitive to Triton X-100 inhibition. In fact, Ca-dependent activities actually increase, while the Q44A Mg-dependent activities are decreased by Triton. However, this inhibitory effect is greatly attenuated as compared to that of the WT (C10S) sample and the other polar residue mutants. Thus, there may be either a component of the inhibitory effect of Triton X-100 that is detected only when assaying for Mg-nucleotidase activities or a stabilizing effect on NTPDase3

Table 1: Characteristics of the Mutants Generated in This Study[a]

NTPDase3 "wt" background or mutant	relative expression level	normalized Mg^{2+}-ATPase (μmol mg^{-1} h^{-1})	% Mg^{2+}-ATPase in Triton X-100	CuPhen cross-linking
Alanine Mutants				
background (C10S)	1	317 ± 27	10 ± 3	–
S33A	0.36 ± 0.07[b]	334 ± 32	14 ± 4	–
S39A	0.26 ± 0.01[b]	327 ± 23	9 ± 2	–
T41A	0.76 ± 0.15	212 ± 51	15 ± 2	–
Q44A	0.58 ± 0.06[b]	97 ± 8[b]	57 ± 2[b]	–
T490A	0.8 ± 0.14	236 ± 9[b]	9 ± 1	–
T495A	0.54 ± 0.11[b]	206 ± 1[b]	7 ± 2	–
C501A	0.41 ± 0.02[b]	329 ± 4	9 ± 1	–
Single-Cysteine Mutants				
background (C10S/C501S/C509S)	1	215 ± 6	11 ± 1	none detected
S33C	0.39 ± 0.09[b]	242 ± 3[b]	9 ± 3	none detected
S39C	0.31 ± 0.05[b]	373 ± 30[b]	9 ± 1	intermolecular
T41C	0.86 ± 0.10	196 ± 16	12 ± 0	intermolecular
Q44C	0.67 ± 0.09[b]	57 ± 2[b]	31 ± 1[b]	quantitatively intermolecular
T490C	0.84 ± 0.03	180 ± 15	17 ± 1[b]	intermolecular
T495C	0.81 ± 0.02	141 ± 17[b]	11 ± 1	intermolecular
C501	0.97 ± 0.13	153 ± 9[b]	10 ± 2	none detected
Double-Cysteine Mutants (potential hydrogen bond pairings)				
background (C10S/C501S/C509S)	1	131 ± 9	9 ± 1	none detected
S39C/T495C	0.31 ± 0.07[b]	61 ± 6[b]	13 ± 1[b]	intermolecular
Q44C/T490C	0.65 ± 0.11[b]	41 ± 6[b]	24 ± 1[b]	intra- and intermolecular
S33C/C501	0.27 ± 0.04[b]	69 ± 2[b]	8 ± 1	quantitatively intramolecular
Q44C Double-Cysteine Mutants (higher-order oligomer formation?)				
background (C10S/C501S/C509S)	1	70 ± 1	12 ± 1	none detected
Q44C	0.65 ± 0.21[b]	32 ± 1[b]	33 ± 1[b]	dimer formation
S39C/Q44C	1.91 ± 0.30[b]	15 ± 1[b]	30 ± 1[b]	higher-order oligomers
T41C/Q44C	1.58 ± 0.29[b]	8 ± 2[b]	57 ± 1[b]	dimer formation
T495C/Q44C	1.27 ± 0.10	22 ± 1[b]	25 ± 1[b]	higher-order oligomers

[a] Different sets of mutations were made in different WT-like NTPDase3 backgrounds, depending on the purpose of the experiment. Because different sets of experiments using the same WT-like background were conducted at different times, and because transfection efficiencies between sets of experiments are variable due to many factors such as slight differences in COS cell confluency at the time of transfection (leading to variations in absolute nucleotidase specific activities), the same NTPDase3 backgrounds are reported here for each set of mutants made. Nucleotidase activities reported for each set of mutants are normalized to the expression level of the WT-like NTPDase3 background used for that set of mutations. [b] Statistically significant ($p \le 0.05$).

mediated by calcium. Nevertheless, the relative insensitivity of the Q44A mutant to Triton inhibition suggests that alanine substitution at Q44 may result in compromised TM helix interactions between two different monomers, presumably accounting for the approximately 70% decrease in Mg-ATPase activity [as compared to that of WT (C10S), each in the absence of detergent], and explaining the attenuation of the further decrease in enzymatic activity after Triton X-100 treatment (Figure 2A). These data suggest that the conserved polar residues in the TMD of NTPDase3 play a pivotal role in normal protein expression and the stability of the TM helix interactions of the native, oligomeric structure of NTPDase3 necessary for full enzymatic activity, with the highly conserved, and strongly polar, Q44 residue playing a dominant role.

Characterization of the Mutants with Polar Residues Singly Mutated to Cysteine. To improve our understanding of the contributions the TMDs make to the oligomeric structure of NTPDase3, it is important to elucidate if, and how, the hydrogen bonds of the conserved polar residues interact between the N- and C-terminal TM helices. This should allow development of a working model for TM helix interactions. A cysteine substitution, disulfide bond formation strategy was utilized to accomplish this goal.

The introduction of a free sulfhydryl by cysteine substitution may cause potential problems for protein folding and processing (due to inappropriate disulfide bond formation), so each polar residue was first singly substituted for cysteine in the "free sulfhydryl-less" C10S/C501S/C509S NTPDase3 background (ensuring that the introduced cysteine is the only free sulfhydryl available for chemical reactivity). All these mutants were enzymatically active (Table 1) and properly processed and trafficked to the cell surface (data not shown). Importantly, like the Q44A mutation, the Q44C mutation decreased specific nucleotidase activities by approximately 70% (Table 1) and was also relatively resistant to Triton X-100 detergent inhibition, unlike the other cysteine mutants (Figure 2B).

To explore the possibility of spontaneous, intermolecular disulfide bond formation via the introduced cysteine residue, the mutants were analyzed by SDS−PAGE with and without reduction by 30 mM DTT. As seen in Figure 3, several of the single-cysteine mutants form some spontaneous, intermolecular disulfide dimers and higher-order oligomers. Via quantitative

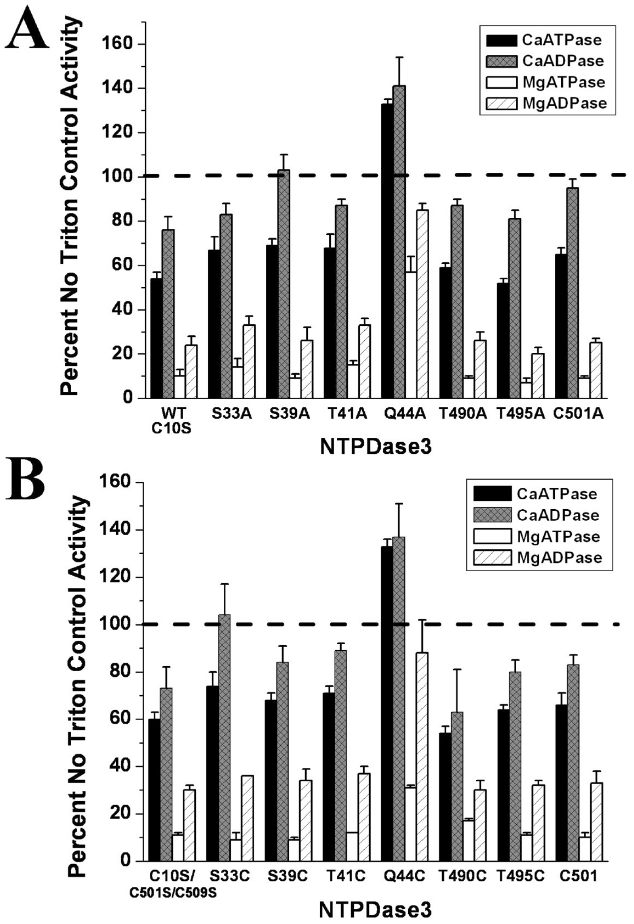

FIGURE 2: Alanine and cysteine substitution at Q44 greatly attenuates the detergent inhibition of NTPDase3 enzymatic activities by Triton X-100. (A) Effect of alanine substitutions on the Triton X-100-treated enzyme activities. (B) Effect of cysteine substitutions on the Triton X-100-treated enzyme activities. The activities are expressed as the percent control activity measured in the absence of Triton X-100. Values represent the mean ± standard deviation from three separate experiments. The dashed horizontal line indicates no change in activity in the presence of Triton X-100.

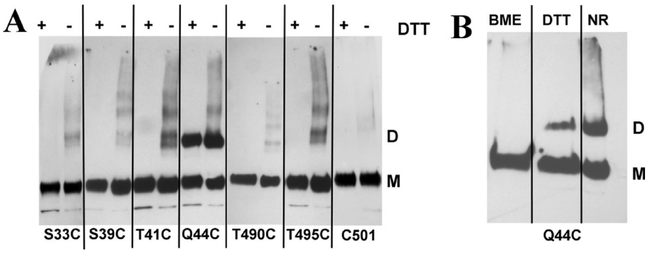

FIGURE 3: Q44C NTPDase3 mutants form spontaneous, intermolecular disulfide bond dimers. (A) Western blot analysis for the presence of spontaneous, intermolecular disulfide bond formation. (B) Analysis of the Q44C intermolecular disulfide-linked dimer which is resistant to reduction by 30 mM DTT (A). The contents of lane BME were boiled for 5 min in 2.86 M (20%) BME. The contents of lane DTT were boiled for 5 min in 200 mM DTT. The contents of lane NR were boiled for 5 min in the absence of reductant. The monomer (M) and dimer (D) bands are labeled. Bands migrating above the dimer are higher-order oligomers.

comparison of the monomer bands of the treated versus untreated samples for each mutant, it is evident that the extent of this spontaneous cross-linking is small for most mutants (it should be noted that the antibody reacts much more strongly with oligomeric forms of NTPDase3 than with monomeric NTPDase3 on Western blots). Furthermore, each of the spontaneously cross-linked cysteine mutants was sensitive to 30 mM DTT reduction, except Q44C. To ensure that the spontaneous cross-linking observed in Q44C was indeed disulfide-mediated, this sample was treated with 200 mM DTT or 2.86 M (20%) β-mercaptoethanol (BME) at 100 °C for 5 min prior to SDS−PAGE. As seen in Figure 3B, the spontaneously dimeric Q44C mutant was still somewhat resistant to reduction by this very high concentration of DTT but was fully reduced by the very high concentration of BME used. These data suggest that Q44 in the N-terminal TM helix of one monomer preferentially intermolecularly interacts with Q44 in the N-terminal helix of the other monomer in dimeric NTPDase3. The spontaneous cross-linking and resistance to DTT reduction of the Q44C mutant demonstrate not only the proper orientation and close proximity needed for effective hydrogen bonding but also the possible presence of a hydrophobic core between the N-terminal TM helices of spontaneously dimeric Q44C.

Paired Cysteine Mutagenesis and Generation of a Model Incorporating the Inter- and Intramolecular Hydrogen Bonding Pattern of the Conserved Polar Residues in the TM Helices of NTPDase3. The helical wheel analysis predicted that Q44 and T490, S39 and T495, and S33 and C501 are on the same helical face and at the same depth in the cell membrane of their respective TM helices (Figure 1B). Thus, in a dimeric structure, these residues have the potential for inter- or intramolecular hydrogen bonding with themselves or each other (Figure 1C). To test this hypothesis, each of the putative polar residue hydrogen bonding pairs was substituted for cysteine residues in the free sulfhydryl-less C10S/C501S/C509S NTPDase3 background [the C10S/C509S background for the S33C/C501 mutant (Table 1)], ensuring that these mutants have only two free cysteines available for sulfhydryl-specific cross-linking via copper phenanthroline (CuPhen) oxidation. Each double mutant cysteine pair was enzymatically active (Table 1). To assess the proximity and orientation of each cysteine residue to one another in the TMD of NTPDase3, and to determine if each pair might preferentially interact via inter- or intramolecular TM helical hydrogen bonds, we alkylated each double-cysteine mutant with maleimide polyethylene glycol 5000 (MalPEG), oxidized each with CuPhen, or treated each with a combination of CuPhen followed by MalPEG. MalPEG reacts covalently to alkylate all free sulfhydryls, adding approximately 5 kDa for each molecule of MalPEG added to NTPDase3 protein. [Under the reaction conditions outlined in Materials and Methods, complete and quantitative MalPEG modifications of C10S NTPDase3, as well as two other mutants containing TM cysteine substitutions, were observed (data not shown).] In each experiment, the double-cysteine mutants were first alkylated with MalPEG, before oxidative cross-linking with CuPhen, to allow differentiation of cysteines present as free sulfhydryls as opposed to those being involved in spontaneous, intramolecular cross-linking.

As seen in Figure 4A, neither the S33C nor the C501 single-cysteine mutant exhibits intermolecular cross-linking (dimer formation) after oxidation with CuPhen. When the S33C/C501 paired cysteine mutant was alkylated with MalPEG, oxidized with CuPhen, or oxidized with CuPhen followed by alkylation with MalPEG, the mutant protein also migrated as a monomer on the SDS−PAGE gel under all conditions. This suggests that the cysteines present at positions 33 and 501 (in the S33C/C501 mutant) are spontaneously and quantitatively, intramolecularly

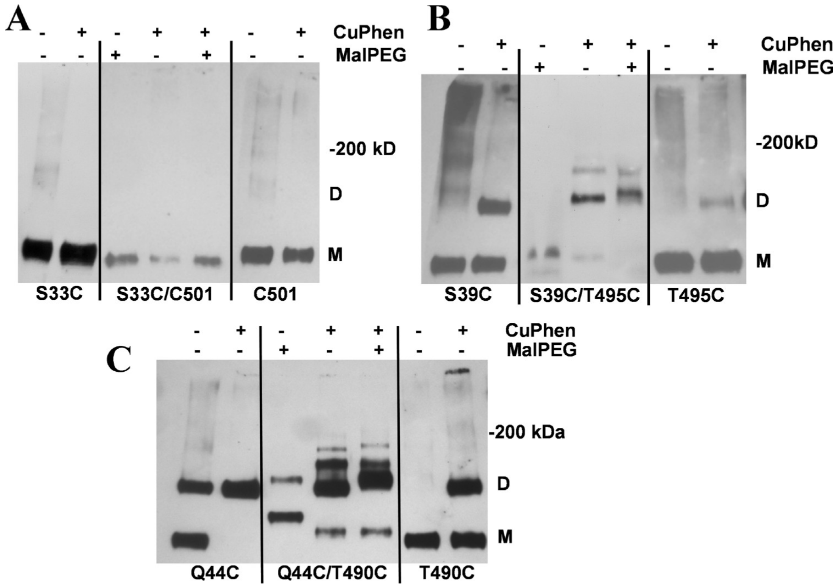

FIGURE 4: Oxidative cross-linking and alkylation of NTPDase3 polar residue hydrogen bonding pair (double cysteine) mutants. (A) Lack of alkylation with MalPEG and lack of CuPhen-induced dimer formation suggesting quantitative, intramolecular cross-linking of the S33C/C501 mutant. (B) CuPhen-induced, intermolecular interactions of the S39C/T495C mutant. (C) Spontaneous inter- and CuPhen-induced, intramolecular interactions of the Q44C/T490C mutant. The monomer (M) and dimer (D) bands are indicated.

cross-linked, and therefore unavailable for exogenous sulfhydryl chemical reactions (i.e., no MalPEG alkylation or CuPhen oxidation occurs).

In Figure 4B, S39C and T495C single-cysteine mutants intermolecularly cross-link to a relatively small extent, with S39C cross-linking more efficiently than T495C. When the S39C/T495C paired cysteine mutant is oxidized with CuPhen, dimers are formed indicating intermolecular cross-linking. Oxidation of the S39C/T495C paired cysteine mutant with CuPhen followed by MalPEG alkylation reiterates the dimer formation, and an electrophoretic shift for the dimer is seen, indicating the presence of free sulfhydryls even after oxidative cross-linking.

In Figure 4C, the Q44C mutant quantitatively cross-links intermolecularly in the presence of CuPhen (i.e., no monomer remains), and the T490C mutant also cross-links intermolecularly, but with a much lower efficiency. When the Q44C/T490C paired cysteine mutant is alkylated with MalPEG alone, two bands are seen with shifted mobilities, indicating the presence of free sulfhydryls in both the monomer and the spontaneously cross-linked dimer. After CuPhen cross-linking, at least four bands are seen. The lowest band indicates intramolecular cross-linking, as evidenced by its electrophoretic shift to a position slightly above the monomer, and the lack of any shift seen after further alkylation with MalPEG. The most dense band, second from the bottom, represents the spontaneously and CuPhen-induced, intermolecularly cross-linked Q44C dimer, which contains two free sulfhydryls, since after MalPEG alkylation it migrates at approximately 10 kDa higher than the spontaneous and CuPhen-induced Q44C dimer. The third band from the bottom represents a dimer which is apparently intermolecularly cross-linked between both the N-terminal (Q44C/Q44C) and C-terminal (T490C/T490C) TM helices of two monomers. After alkylation with MalPEG, the electrophoretic mobility of the band (third from the bottom) does not change as compared with it being oxidized with CuPhen alone. The faint fourth band from the bottom may represent a higher-order oligomer.

Integrating all the cross-linking data leads to the putative hydrogen bonding pattern of the conserved polar residues as illustrated in Figure 5. The polar residues mutated, the labeling of the monomer 1 helices [denoted as N1 (N-terminal domain) and C1 (C-terminal domain)] and the solid lines representing the inter- and intramolecular interactions of monomer 1, are shown in bold. Monomer 2, containing TM helices denoted N2 and C2, and the dotted lines representing the intramolecular interactions of monomer 2 are labeled without bolding. The black circles represent the polar residues with the circle size decreasing as each amino acid increases in depth in the cell membrane from the extracellular surface (see the legend of Figure 1 for a complete description of the representations in panel A). This model places S39, T495, and, to a lesser extent, T41 on the "outside" of the interacting faces of the TM helices forming dimeric NTPDase3 (i.e., they are not directly involved in making TM polar dimeric contacts). To test this model, which suggests that S39, T495, and possibly T41 are not involved in hydrogen bonding within a dimer but may instead be involved in higher-order oligomer interactions involving multiple dimers, we used site-directed mutagenesis to make Q44C/S39C, Q44C/T41C, and Q44C/T495C double-cysteine mutants. Our hypothesis was that upon oxidative cross-linking by CuPhen, these "outside-facing" polar residues, coupled with the spontaneously, intermolecularly cross-linked Q44C mutant (revealing the natural dimer), could form higher-order oligomers. Each of these double-cysteine mutants was enzymatically active (Table 1) and properly processed and trafficked to the cell surface (data not shown). As seen in Figure 6, the Q44C/S39C mutant (and, to a lesser extent, the Q44C/T495C mutant) forms a small amount of higher-order oligomers (above 200 kDa, indicated by asterisks), and these bands do not electrophoretically shift upon addition of MalPEG, suggesting the absence of free sulfhydryls. No higher-order oligomers are evident after oxidative cross-linking of the Q44C/T41C mutant. These data suggest that while Q44 is a main player in driving the association of the TM helices of dimeric NTPDase3, S39, and possibly T495, may contribute to the formation of higher-order oligomers. T41 does not seem to play a role in promoting higher-order oligomerization but instead is most likely teamed with Q44 to form a "polar-X-X-polar" (T41-X-X-Q44) motif mediating TM helix association (*41*, *42*).

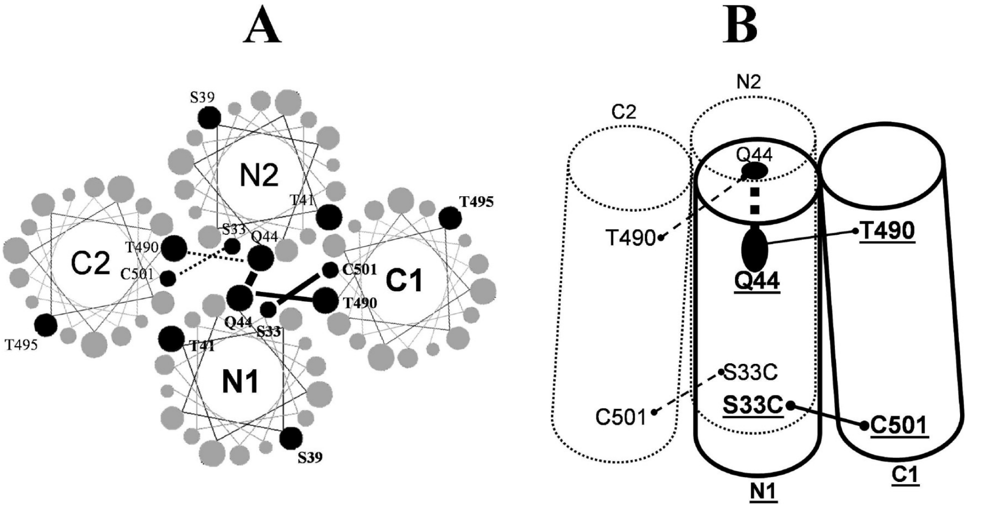

FIGURE 5: Model of the putative TMD hydrogen bond helical interactions in the NTPDase3 dimer. (A) Helical wheel model depicting the putative inter- and intramolecular hydrogen bonding pattern of the conserved polar residues in the TMD of NTPDase3. (B) Three-dimensional model depicting the putative inter- and intramolecular hydrogen bonding pattern of the conserved polar residues in the TMDs of NTPDase3. In the figure, the tops of the helical cylinders are at the interface between the cell membrane and the extracellular portion of the NTPDase containing the active site. Monomer 1, denoted as N1 (N-terminal helix) and C1 (C-terminal helix), is represented as solid cylinders with polar residues important for dimer interactions underlined and solid lines representing the hydrogen bond helical interactions. Monomer 2, with the TM helices denoted as N2 and C2, is represented as dotted cylinders with dotted lines representing the hydrogen bond helical interactions.

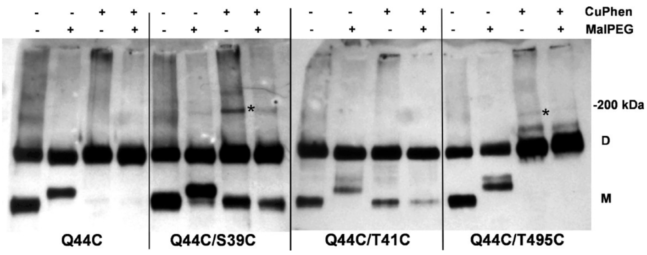

FIGURE 6: S39C and T495C may participate in hydrogen bond interactions involved in the formation of tetrameric NTPDase3. The mutants were oxidized with CuPhen and alkylated with MalPEG as described in Materials and Methods. Unlike the parent Q44C, a small amount of higher-order oligomers is observed in the S39C/Q44C and T495C/Q44C double-cysteine mutants. The monomer (M) and dimer (D) bands are labeled, and the positions of the higher-order oligomers observed for Q44C/S39C and Q44C/T495C are indicated with asterisks.

Tween 20 Stimulation of NTPDase3. The NTPDases, including human NTPDase3 utilized in this work, are generally inhibited by most detergents used to solubilize membrane-bound proteins (*8*). During the course of this study, we discovered that incubation of NTPDase3 with 0.1% Tween 20 increases the Mg-ATPase activity of the human enzyme by more than 2.5-fold and inhibits the enzymatic activity of human NTPDase1 and -2 by ~50−70% (Figure 7A), indicating the stimulation of activity by Tween 20 is selective for NTPDase3. Similar 2.5−3-fold Tween 20 NTPDase3 stimulatory effects were also seen via measurement of Mg-ADPase activity and Ca-dependent nucleotidase activities (data not shown). In addition, Figure 7B shows that incubation of human, mouse, and rat NTPDase3 with 0.1% Tween 20 results in a >2.5-fold increase in Mg-ATPase activity, indicating the stimulatory effect is not species-specific.

We hypothesized the detergent Tween 20 stimulates the enzyme activity of NTPDase3 by enhancing the oligomeric stability of the enzyme, mediated by the TMDs. Glutaraldehyde (a lysine-specific cross-linker) has been frequently used to assess the oligomerization status of the NTPDases (*43*). NTPDase3 (WT-like C10S) was therefore glutaraldehyde cross-linked in the absence of any detergent, as well as after treatment with 0.1% of the detergent digitonin, Tween 20, or Triton X-100, and analyzed on a reducing SDS−PAGE gel. As seen in Figure 8A, NTPDase3 treated with digitonin [which maintains activity and native oligomeric structure (*8*)] resulted in efficient cross-linking into dimers and higher-order oligomers. NTPDase3 treated with Tween 20 resulted in more dimer and higher-order oligomer formation, and less monomer remaining following glutaraldehyde cross-linking as compared to the NTPDase3 treated with no detergent or treated with digitonin. In contrast, NTPDase3 treated with Triton X-100 dramatically decreased the cross-linking efficiency of the normally dimeric NTPDase3 (presumably by abolishing oligomer formation). These data suggest Tween 20, unlike Triton X-100 (and most other detergents), enhances NTPDase3 oligomer formation, resulting in increased nucleotidase activity.

Detergents generally have their inhibitory effects on the membrane-bound NTPDase enzymes but do not inhibit the soluble, extracellular domains of these same enzymes (*16*). To test the hypothesis that NTPDase3 Tween 20 stimulation of activity is mediated by the TMD, a soluble NTPDase3 construct (lacking the TM helices and short cytoplasmic N- and C-terminal tails) was treated with Tween 20 to assess its effect on activity. No change in soluble NTPDase3 activity was observed (data not shown), indicating the Tween 20 stimulatory effect is indeed mediated by the TMD of NTPDase3. The S39C/T495C double-cysteine mutant was used to further test the hypothesis that Tween 20 increases the enzymatic activity of NTPDase3 by promoting oligomerization at the TMD level. The S39C/T495C mutant protein (in the free sulfhydryl-less NTPDase3 background) was treated with or without 0.1% Tween 20 or Triton X-100, followed by oxidative cross-linking with a final CuPhen concentration of 0.5 mM for 20 min at 37 °C. As seen in Figure 8B, treatment of the S39C/T495C mutant with 0.1% Tween 20 followed by CuPhen cross-linking resulted in the monomeric enzyme being efficiently, intramolecularly cross-linked (upward shift of monomer band) and more

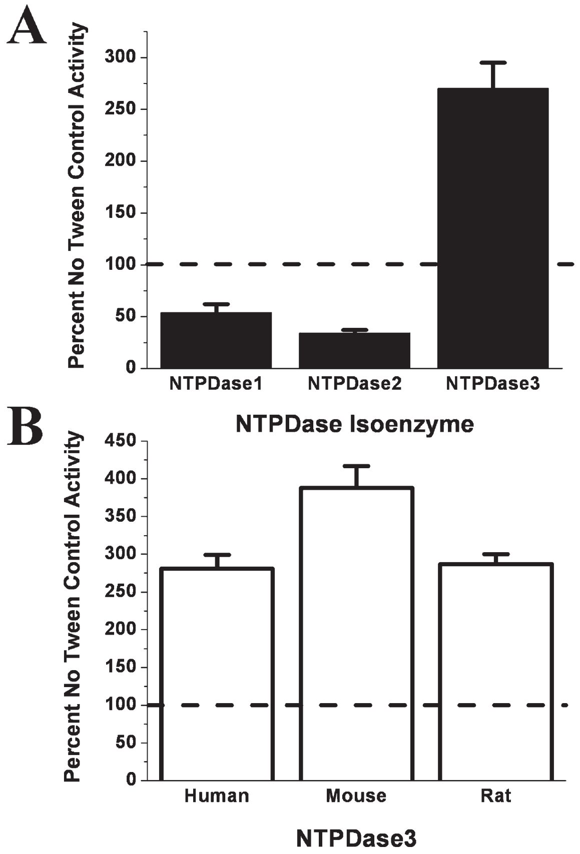

FIGURE 7: Stimulatory effect of Tween 20 that is specific for NTPDase3 and conserved among species. (A) Mg-ATPase assay of human, membrane-bound NTPDase isoenzymes in the presence of 0.1% Tween 20. (B) Mg-ATPase assay of NTPDase3 from three species in the presence of 0.1% Tween 20. The activities are expressed as the percent control activity measured in the absence of Tween 20. Values represent the mean ± standard deviation from three separate experiments. The dashed horizontal lines indicate no change in activity in the presence of Tween 20.

efficiently, intermolecularly cross-linked to oligomeric forms. On the other hand, 0.1% Triton X-100 treatment of S39C/T495C followed by CuPhen oxidation resulted in elimination of dimer and higher-order oligomer formation, with intramolecular (within a monomer) cross-linking still evident as an upward shift in the electrophoretic mobility of the monomer. Thus, the NTPDase3-selective stimulatory effect of Tween 20 might be explained by this detergent promoting oligomerization via the TM helices of NTPDase3, which contain a set of unique, conserved polar residues not present in NTPDase1 or NTPDase2.

DISCUSSION

Polar residues play essential roles in protein stability, function, and TM helical association via hydrogen bonding (*44−51*). The conservation of the polar residues in the TMD of human NTPDase3 suggests their participation in the formation of hydrogen bonds important for the structure and function of the enzyme. Knowledge of the role of these conserved polar residues, their hydrogen bond interactions, and resulting TM helical arrangement is necessary for understanding the functional effects of oligomerization of NTPDase3 and its modulation by membrane perturbation. Therefore, we singly mutated the polar residues to alanine and analyzed the effect of eliminating each polar residue in the TM helices of NTPDase3. Then we mutated the polar residues to cysteine, both singly and in pairs, in a free sulfhydryl-less NTPDase3 background (C10S/C501S/C509S NTPDase3) to elucidate possible hydrogen bonding pairs involving these residues.

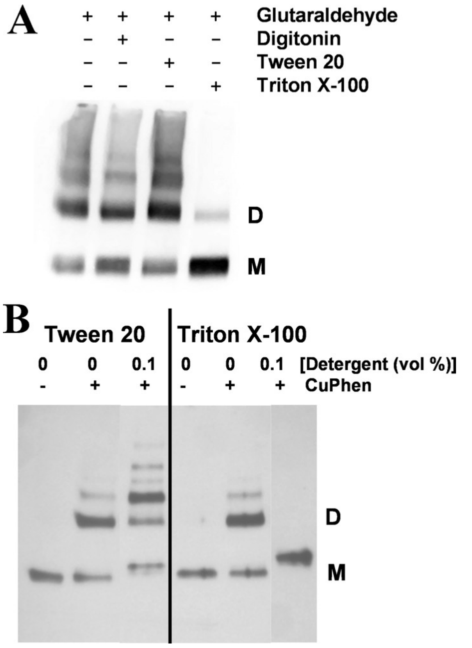

FIGURE 8: Tween 20 promotes oligomerization mediated by the TM helices of NTPDase3. (A) Effect of Tween 20 on glutaraldehyde (lysine-specific) cross-linking efficiency via the nontransmembrane regions of C10S (WT-like) NTPDase3. Note that there is less monomer remaining, and more oligomers formed, in the presence of Tween 20, in sharp contrast to the large attenuation of cross-linking observed with Triton X-100 detergent. (B) Effect of 0.1% Tween 20 or Triton X-100 on CuPhen cross-linking efficiency of the TM helices of the S39C/T495C double-cysteine NTPDase3 mutant. Note the stark contrast in the intermolecular cross-linking efficiencies obtained using Tween 20 vs Triton X-100 as the detergent.

Our data strongly suggest the conserved polar residues in the TM helices of human NTPDase3 are important for optimal protein expression and enzymatic activity (Table 1), presumably by forming hydrogen bonds necessary for proper protein folding and association of TM helical interactions as demonstrated by our disulfide cross-linking strategy. Interestingly, the Q44A and Q44C mutants exhibited similar enzymatic characteristics (Table 1 and Figure 2), namely, a decrease in nucleotidase activities and the elimination of the Ca-nucleotidase inhibition and attenuation of the Mg-nucleotidase inhibition by Triton X-100 [Triton X-100, as well as many other detergents, has been shown to inhibit the activity of NTPDase3 as well as most other cell surface NTPDases (*8*)]. Presumably, these mutations disrupted the inter- and intramolecular (glutamine, a strongly polar residue, can form two hydrogen bonds) hydrogen bonding pattern necessary for proper TM helical association (Figure 4C). The spontaneous, intermolecular disulfide bond formation observed in the Q44C mutant [resistant to even very high concentrations of DTT but could be reduced by high concentrations of the more hydrophobic reduction agent, BME (Figure 3B)] most likely limits the dynamic motions of the TM helices. This decreases activity, since both appropriate hydrogen bonding and movement of the TM helices during nucleotide hydrolysis are necessary to achieve full enzymatic activity (Table 1). This suggests that residue Q44 of one monomer is in the proximity and in the correct orientation with respect to Q44 of the other monomer in a dimer, and that the N-terminal TM helices of dimeric NTPDase3 interact efficiently near the extracellular surface of the cell membrane. The current data demonstrating the importance of the strongly polar Q44 residue, which is located at the interface of the N-terminal TM helix with the extracellular portion of NTPDase3, are consistent with data published by Grinthal and Guidotti (*32*) using rat NTPDase1. In that earlier study, those authors, through cysteine substitution and oxidative cross-linking, identified strong inter- and intramolecular interactions between the TM helices of NTPDase1 involving residues near the extracellular surface of the membrane and further demonstrated formation of a disulfide bond between two transmembrane helices decreased enzymatic activity.

The S33C/C501 double-cysteine mutant appears to spontaneously and completely form intramolecular disulfides [cross-linking between TM helices within a monomer (Figure 4A)], while the S39C/T495C mutant appears to form intermolecular disulfides (Figure 4B). These cross-linking data suggest the putative hydrogen bonding pattern of the conserved polar residues as illustrated in Figure 5 that places S39, T495, and T41 on the outside of the TM helices forming dimeric NTPDase3. In turn, this suggests that S39, T495, and/or T41 could be involved in higher-order oligomer interactions [e.g., to form the “dimer of dimers” (*35*)]. As seen in Figure 6, the Q44C/S39C (and to a lesser extent the Q44C/T495C) mutant forms a small amount of higher-order oligomers above 200 kDa, presumably tetramers. Taken together, these cross-linking results suggest that Q44 is the linchpin residue in the association of the TM helices to form dimeric NTPDase3 and that S39 (and possibly T495) may form intermolecular hydrogen bonds to promote interactions that facilitate formation of the tetrameric and higher-order oligomeric forms of NTPDase3 (Figure 5). Lastly, T41, because of its inability to form higher-order oligomers when combined with Q44C (Figure 6), is not likely to be directly involved in higher-order oligomer formation (as depicted in Figure 5A by its relative inaccessibility) but instead may work in concert with Q44 to provide the specificity of the N-terminal helix associations in the dimeric polar-X-X-polar (T41-X-X-Q44) TM−TM association motif (*52*).

During the course of this study, we also discovered a species-conserved, stimulatory effect of Tween 20 on the nucleotidase activities of NTPDase3 (Figure 7B) that may facilitate future structural studies and serve as a useful tool for identifying the presence and importance of NTPDase3 in various tissues and processes. Considering this stimulatory effect is isoenzyme-specific, not observed in the closely related human NTPDase1 or NTPDase2 (Figure 7A), it is not unlikely that the unique TMD hydrogen bond interactions mediated by the conserved polar residues of NTPDase3 promote the association of the TM helices (Figure 8B) in the presence of Tween 20.

The conserved NTPDase3 TMD polar residues examined here are not conserved in other membrane-bound NTPDases, suggesting that the results reported here are specific for this isoenzyme, and that other NTPDases have different mechanisms and amino acids facilitating TM helix interactions and oligomeric associations. It is likely that this partially explains the differential susceptibility to membrane perturbation (e.g., detergent activation and inactivation) (*53*, *54*) and substrate specificities (*7*, *55*) seen in different family members of the NTPDase enzymes.

ACKNOWLEDGMENT

We thank Dr. Vasily Ivanenkov in our laboratory for making the original observation of the stimulatory effect of Tween 20 on NTPDase3.

REFERENCES

1. Zimmermann, H., Beaudoin, A. R., Bollen, M., Goding, J. W., Guidotti, G., Kirley, T. L., Robson, S. C., and Sano, K. (1999) in Second International Workshop on Ecto-ATPases and Related Ectonucleotidases (Vanduffel, L., Ed.) pp 1−9, Shaker Publishing BV, Maastricht, The Netherlands.
2. Zimmermann, H. (1999) Two novel families of ectonucleotidases: Molecular structures, catalytic properties and a search for function. *Trends Pharmacol. Sci. 20*, 231–236.
3. Wang, T.-F., and Guidotti, G. (1998) Golgi Localization and Functional Expression of Human Uridine Diphosphatase. *J. Biol. Chem. 273*, 11392–11399.
4. Ivanenkov, V. V., Meller, J., and Kirley, T. L. (2005) Characterization of Disulfide Bonds in Human Nucleoside Triphosphate Diphosphohydrolase 3 (NTPDase3): Implications for NTPDase Structural Modeling. *Biochemistry 44*, 8998–9012.
5. Ivanenkov, V. V., Murphy-Piedmonte, D. M., and Kirley, T. L. (2003) Bacterial Expression, Characterization, and Disulfide Bond Determination of Soluble Human NTPDase6 (CD39L2) Nucleotidase: Implications for Structure and Function. *Biochemistry 42*, 11726–11735.
6. Murphy-Piedmonte, D. M., Crawford, P. A., and Kirley, T. L. (2005) Bacterial Expression, Folding, Purification and Characterization of Soluble NTPDase5 (CD39L4) Ecto-nucleotidase. *Biochim. Biophys. Acta 1747*, 251–259.
7. Kukulski, F., Lévesque, S. A., Lavoie, E. G., Lecka, J., Bigonnesse, F., Knowles, A. F., Robson, S. C., Kirley, T. L., and Sévigny, J. (2005) Comparative hydrolysis of P2 receptor agonists by NTPDases 1, 2, 3 and 8. *Purinergic Signalling 1*, 193–204.
8. Plesner, L. (1995) Ecto-ATPases: Identities and functions. *Int. Rev. Cytol. 158*, 141–214.
9. Kirley, T. L., Crawford, P. A., and Smith, T. M. (2006) The structure of the nucleoside triphosphate diphosphohydrolases (NTPDases) as revealed by mutagenic and computational modeling analysis. *Purinergic Signalling 2*, 379–389.
10. Zebisch, M., and Sträter, N. (2008) Structural insight into signal conversion and inactivation by NTPDase2 in purinergic signaling. *Proc. Natl. Acad. Sci. U.S.A. 105*, 6882–6887.
11. Zebisch, M., and Sträter, N. (2007) Characterization of Rat NTPDase1, -2, and -3 ectodomains refolded from bacterial inclusion bodies. *Biochemistry 46*, 11945–11956.
12. Gayle, R. B., Maliszewski, C. R., Gimpel, S. D., Schoenborn, M. A., Caspary, R. G., Richards, C., Brasel, K., Price, V., Drosopoulos, J. H. F., Islam, N., Alyonycheva, T. N., Broekman, M. J., and Marcus, A. J. (1998) Inhibition of Platelet Function by Recombinant Soluble Ecto-ADPase/CD39. *J. Clin. Invest. 101*, 1851–1859.
13. Treuheit, M. J., Vaghy, P. L., and Kirley, T. L. (1992) The Mg^{2+}-ATPase of rabbit skeletal muscle transverse tubules is a 67 kDa glycoprotein. *J. Biol. Chem. 267*, 11777–11782.
14. Failer, B. U., Aschrafi, A., Schmalzing, G., and Zimmermann, H. (2003) Determination of native oligomeric state and substrate specificity of rat NTPDase1 and NTPDase2 after heterologous expression in *Xenopus* oocytes. *Eur. J. Biochem. 270*, 1802–1809.
15. Smith, T. M., and Kirley, T. L. (1999) Glycosylation is essential for functional expression of a human brain ecto-apyrase. *Biochemistry 38*, 1509–1516.
16. Wang, T. F., Ou, Y., and Guidotti, G. (1998) The transmembrane domains of ectoapyrase (CD39) affect its enzymatic activity and quaternary structure. *J. Biol. Chem. 273*, 24814–24821.
17. Landolt-Marticorena, C., Williams, K. A., Deber, C. M., and Reithmeier, R. A. (1993) Non-random distribution of amino acids in the transmembrane segments of human type I single span membrane proteins. *J. Mol. Biol.* 602–608.
18. Tourasse, N. J., and Li, W. H. (2000) Selective constraints, amino acid composition, and the rate of protein evolution. *Mol. Biol. Evol.,* 656–664.
19. Eilers, M., Shekar, S. C., Shieh, T., Smith, S. O., and Fleming, P. J. (2000) Internal packing of helical membrane proteins. *Proc. Natl. Acad. Sci. U.S.A. 97*, 5796–5801.
20. Partridge, A. W., Therien, A. G., and Deber, C. M. (2002) Polar mutations in membrane proteins as a biophysical basis for disease. *Biopolymers 66*, 350–358.
21. Partridge, A. W., Therien, A. G., and Deber, C. M. (2004) Missense mutations in transmembrane domains of proteins: Phenotypic propensity of polar residues for human disease. *Proteins 54*, 648–656.
22. Adamian, L., and Liang, J. (2003) Interhelical hydrogen bonds in transmembrane region are important for function and stability of Ca^{2+}-transporting ATPase. *Cell Biochem. Biophys. 39*, 1–12.

23. White, S. H., and Wimley, W. C. (1999) Membrane protein folding and stability: Physical principles. *Annu. Rev. Biophys. Biomol. Struct. 28*, 319–365.
24. Adamian, L., and Liang, J. (2002) Interhelical hydrogen bonds and spatial motifs in membrane proteins: Polar clamps and serine zippers. *Proteins 47*, 209–218.
25. Lynch, B. A., and Koshland, D. E. J. (1991) Disulfide crosslinking studies of the transmembrane regions of the aspartate sensory receptor of *Escherichia coli*. *Proc. Natl. Acad. Sci. U.S.A. 88*, 10402–10406.
26. Pakula, A. A., and Simon, M. I. (1992) Determination of transmembrane protein structure by disulfide crosslinking: The *Escherichia coli* Tar receptor. *Proc. Natl. Acad. Sci. U.S.A. 89*, 4144–4148.
27. Whitley, P., Nilsson, L., and von Heijne, G. (1993) Three-dimensional model of the membrane domain of *Escherichia coli* leader peptidase based on disulfide mapping. *Biochemistry 32*, 8534–8539.
28. Duche, D., Parker, M. W., Gonzalez-Manas, J. M., Pattus, F., and Baty, D. (1994) Uncoupled steps of the colicin A pore formation demonstrated by disulfide bond engineering. *J. Biol. Chem. 269*, 6332–6339.
29. Lee, G. F., Burrows, G. G., Lebert, M. R., Dutton, D. P., and Hazelbauer, G. L. (1994) Deducing the organization of a transmembrane domain by disulfide cross-linking: The bacterial chemoreceptor Trg. *J. Biol. Chem. 269*, 29920–29927.
30. Chervitz, S. A., and Falke, J. J. (1995) Lock on/off disulfides identify the transmembrane signaling helix of the aspartate receptor. *J. Biol. Chem. 270*, 24043–24053.
31. Maruyama, I. N., Mikawa, Y. G., and Marayama, H. I. (1995) A model for transmembrane signaling by the aspartate receptor based on random-cassette mutagenesis and site-directed disulfide crosslinking. *J. Mol. Biol. 253*, 530–546.
32. Grinthal, A., and Guidotti, G. (2004) Dynamic Motions of CD39 Transmembrane Domains Regulate and Are Regulated by the Enzymatic Active Site. *Biochemistry 43*, 13849–13858.
33. Chiang, W. C., and Knowles, A. F. (2008) Inhibition of human NTPDase 2 by modification of an intramembrane cysteine by p-chloromercuriphenylsulfonate and oxidative cross-linking of the transmembrane domains. *Biochemistry 47*, 8775–8785.
34. Smith, T. M., and Kirley, T. L. (1999) Site-Directed Mutagenesis of a Human Brain Ecto-Apyrase: Evidence that the E-type ATPases are related to the Actin/Heat Shock 70/Sugar Kinase Superfamily. *Biochemistry 38*, 321–328.
35. Murphy, D. M., Ivanenkov, V. V., and Kirley, T. L. (2002) Identification of Cysteine Residues Responsible for Oxidative Cross-linking and Chemical Inhibition of Human Nucleoside Triphosphate Diphosphohydrolase 3. *J. Biol. Chem. 277*, 6162–6169.
36. Smith, T. M., and Kirley, T. L. (1998) Cloning, sequencing, and expression of a human brain ecto-apyrase related to both the ecto-ATPases and CD39 ecto-apyrases. *Biochim. Biophys. Acta 1386*, 65–78.
37. Stoscheck, C. M. (1987) Protein assay sensitive at nanogram levels. *Anal. Biochem. 160*, 301–305.
38. Fiske, C. H., and Subbarow, Y. (1925) The colorometric determination of phosphorous. *J. Biol. Chem. 66*, 375–400.
39. Baykov, A. A., Evtushenko, O. A., and Avaeva, S. M. (1988) A malachite green procedure for orthophosphate determination and its use in alkaline phosphatase-based enzyme immunoassay. *Anal. Biochem. 171*, 266–270.
40. Careaga, C. L., and Falke, J. J. (1992) Thermal motions of surface α-helices in the D-galactose chemosensory receptor. Detection by disulfide trapping. *J. Mol. Biol. 226*, 1219–1235.
41. Sal-Man, N., Gerber, D., and Shai, Y. (2005) The identification of a minimal dimerization motif QXXS that enables homo- and hetero-association of transmembrane helices in vivo. *J. Biol. Chem. 280*, 27449–27457.
42. Sal-Man, N., Gerber, D., and Shai, Y. (2004) The composition rather than position of polar residues (QxxS) drives aspartate receptor transmembrane domain dimerization in vivo. *Biochemistry 43*, 2309–2313.
43. Murphy, D. M., and Kirley, T. L. (2003) Asparagine 81, an Invariant Glycosylation Site Near Apyrase Conserved Region 1, is Essential for Full Enzymatic Activity of Ecto Nucleoside Triphosphate Diphosphohydrolase 3. *Arch. Biochem. Biophys. 413*, 107–115.
44. Basu, S., Jala, V. R., Mathis, S., Rajagopal, S. T., Del Prete, A., Maturu, P., Trent, J. O., and Haribabu, B. (2007) Critical role for polar residues in coupling leukotriene B4 binding to signal transduction in BLT1. *J. Biol. Chem. 282*, 10005–10017.
45. Zhang, D. W., Nunoya, K., Vasa, M., Gu, H. M., Theis, A., Cole, S. P., and Deeley, R. G. (2004) Transmembrane helix 11 of multidrug resistance protein 1 (MRP1/ABCC1): Identification of polar amino acids important for substrate specificity and binding of ATP at nucleotide binding domain 1. *Biochemistry 43*, 9413–9425.
46. Jelínkova, I., Vávra, V., Jindrichova, M., Obsil, T., Zemkova, H. W., Zemkova, H., and Stojilkovic, S. S. (2008) Identification of P2X(4) receptor transmembrane residues contributing to channel gating and interaction with ivermectin. *Pfluegers Arch. 456*, 939–950.
47. Zhang, D. W., Nunoya, K., Vasa, M., Gu, H. M., Cole, S. P., and Deeley, R. G. (2006) Mutational analysis of polar amino acid residues within predicted transmembrane helices 10 and 16 of multidrug resistance protein 1 (ABCC1): Effect on substrate specificity. *Drug Metab. Dispos. 34*, 539–546.
48. Arkin, I. T. (2002) Structural aspects of oligomerization taking place between the transmembrane α-helices of bitopic membrane proteins. *Biochim. Biophys. Acta 1565*, 347–363.
49. Pogozheva, I. D., Lomize, A. L., and Mosberg, H. I. (1998) Opioid receptor three-dimensional structures from distance geometry calculations with hydrogen bonding constraints. *Biophys. J. 75*, 612–634.
50. Cheung, J. C., and Deber, C. M. (2008) Misfolding of the cystic fibrosis transmembrane conductance regulator and disease. *Biochemistry 47*, 1465–1473.
51. DeGrado, W. F., Gratkowski, H., and Lear, J. D. (2003) How do helix-helix interactions help determine the folds of membrane proteins? Perspectives from the study of homo-oligomeric helical bundles. *Protein Sci. 12*, 647–665.
52. Senes, A., Ubarretxena-Belandia, I., and Engleman, D. M. (2001) The Cα---H···hydrogen bond: A determinant of stability and specificity in transmembrane helix interactions. *Proc. Natl. Acad. Sci. U.S.A. 98*, 9056–9061.
53. Chiang, W. C., and Knowles, A. F. (2008) Transmembrane domain interactions affect the stability of the extracellular domain of the human NTPDase 2. *Arch. Biochem. Biophys. 472*, 89–99.
54. Mukasa, T., Lee, Y., and Knowles, A. F. (2005) Either the carboxyl- or the amino-terminal region of the human ecto-ATPase (E-NTPDase 2) confers detergent and temperature sensitivity to the chicken ecto-ATP-diphosphohydrolase (E-NTPDase 8). *Biochemistry 44*, 11160–11170.
55. Grinthal, A., and Guidotti, G. (2002) Transmembrane Domains Confer Different Substrate Specificities and Adenosine Diphosphate Hydrolysis Mechanisms on CD39, CD39L1, and Chimeras. *Biochemistry 41*, 1947–1956.